

# Preparation of cotton cellulose nanofibers/ZnO/CdS nanocomposites and its photocatalytic activity

Jing Li<sup>1</sup> · Jun Cao<sup>1</sup> · Xiufang Zhang<sup>1</sup> · Song Wang<sup>1</sup> · Yingying Zheng<sup>1</sup> · Jiaqi Pan<sup>1</sup> · Chaorong Li<sup>1</sup>

Received: 16 September 2015 / Accepted: 16 October 2015 / Published online: 22 October 2015  
© Springer Science+Business Media New York 2015

**Abstract** The ZnO/CdS nanocomposites have been successfully synthesized on the electrospun cotton cellulose nanofibers (CCNFs). ZnO nanorods (70–80 nm in diameter and 1 μm in length) are uniformly grown on the CCNFs by a simple hydrothermal method firstly and then different amount of CdS nanoparticles (20–30 nm in diameter) are loaded on the ZnO nanorods by the chemical bath deposition method. The visible light photocatalytic activity of ZnO/CdS nanocomposites is investigated by degradation of Rhodamine B under visible light irradiation, and it demonstrates that the photocatalytic performance of this composites is significantly enhanced compared with that of pure ZnO. Furthermore, the relatively narrow band gap and novel nanostructure of the composites are considered as the main reasons of this enhancement.

## 1 Introduction

Cotton cellulose is the most abundant natural resources on earth and has attracted much attention because of its outstanding properties, such as thermally stable, good flexibility, lightweight and inexpensive [1]. Particularly, the electrospun cotton cellulose nanofibers (CCNFs) have a large specific surface area, which can be used as a kind of good carrier to load other functional nanomaterials. So far, various devices such as thin-film transistors, lithium-ion batteries, active-matrix organic light-emitting displays, and sensors have been fabricated on the cellulose paper

substrates [2–7], such as Sang-Woo Kim et al. [8] used cellulose as a thermally stable, foldable and inexpensive substrate material to get electrical output nanogenerators.

On the other hand, as the increasingly environmental pollution many researchers have been devoted to the study for the degradation of pollutants. However, most of the photocatalysts are limited by the dispersibility, because the agglomeration of powdery photocatalysis can lead the decrease of the photocatalytic efficiency. What's more, the recycling of the powdery photocatalyst is another important factor. Using suitable substrate to load and disperse photocatalysts is an effective way to solve these problems. In our previous work, CCNFs with lightweight and large specific surface area were successfully prepared, which is helpful to photocatalytic activity [9–11]. As know, ZnO is an excellent semiconductor material with the properties of high electron mobility and nontoxicity, which can be used as photocatalyst to degrade the organic pollutants from water under ultraviolet (UV) light irradiation [12–14]. As a pity, owing to its large band gap (3.37 eV), the photocatalytic activity of ZnO is restricted in UV region, which only accounts for about 4 % of the entire solar spectrum. In order to extend the light response region of the ZnO in the visible light region, narrow band gap materials can be introduced on the surface of ZnO to form heterojunction structure. CdS is a well-known semiconductor that has been used as a visible-light photosensitizer because of its narrow direct band gap (2.4 eV). Peng et al. [15] have successfully used CdS quantum dots to sensitize TiO<sub>2</sub> Nanotube-Array as photoelectrode, which exhibits significant photocurrent and efficiency.

In this paper, the binary catalyst ZnO/CdS on the CCNFs with excellent photocatalytic activity were prepared by a facile two-step method. Furthermore, the mechanism of enhancement of high visible photocatalytic activity were also investigated.

✉ Chaorong Li  
crli@zstu.edu.cn

<sup>1</sup> Department of Physics, Key Laboratory of ATMMT Ministry of Education, Zhejiang Sci-Tech University, Hangzhou 310018, People's Republic of China

## 2 Experimental

### 2.1 Chemicals and materials

Cotton linters cellulose (DP = 12,000) was got from Zhejiang Academy of Agricultural Sciences. Methanol (CH<sub>3</sub>OH, ≥99.5 %, AR), anhydrous ethanol (C<sub>2</sub>H<sub>5</sub>OH, ≥99.7 %, AR) were purchased from Hangzhou GaoJing Chemical Reagent Co., Ltd. The N,N-dimethylacetamide (DMAc, ≥99.5 %, AR), hexamethylene tetramine (HMTA, ≥99.0 %, AR), zinc nitrate (Zn(NO<sub>3</sub>)<sub>2</sub>·6H<sub>2</sub>O, ≥99.0 %, AR), zinc acetate (Zn(CH<sub>3</sub>COO)<sub>2</sub>·2H<sub>2</sub>O, ≥99.0 %, AR) were supplied by Tianjin YongDa Chemical Reagent Development Center. Lithium chloride (LiCl, ≥99.5 %, AR), cadmium nitrate tetrahydrate (Cd(NO<sub>3</sub>)<sub>2</sub>·4H<sub>2</sub>O, ≥99.0 %, AR), thioacetamide (TAA, ≥99.0 %, AR) were purchased from Aladdin Reagent Co., Ltd. The cotton and chemicals were used without further purification, but LiCl was preprocessed to remove the water.

### 2.2 Preparation of CCFNs/ZnO/CdS Nanocomposites

CCFNs were obtained by electrospinning process according to our previous work [9]. The growth of ZnO nanorod array has been achieved by hydrothermal synthetic method. Firstly, the cotton cellulose nanofibers were drop-coated 20 times with 15 mM zinc acetate (Zn(CH<sub>3</sub>COO)<sub>2</sub>·2H<sub>2</sub>O) ethanol solution and annealed at 150 °C for 3 h to get the ZnO seed layer. Then, the CCFNs with ZnO seed layer was placed in a 30 ml autoclave containing an aqueous solution of 25 mM Zn(NO<sub>3</sub>)<sub>2</sub>·6H<sub>2</sub>O and 25 mM HMTA. The autoclave was sealed in an electric oven under 90 °C for 10 h. Finally, CdS nanoparticles were deposited on CCFNs/ZnO by the chemical bath deposition (CBD) method [15]. CBD is one of the best methods for the deposition of CdS nanoparticle on other materials because of its simplicity and uniform deposition [16]. The as-prepared CCFNs/ZnO were immersed in an aqueous solution with different concentration of Cd(NO<sub>3</sub>)<sub>2</sub>·4H<sub>2</sub>O (0.001 M, 0.0025 M, 0.005 M, 0.01 M) and corresponding stoichiometric amount TAA (0.001 M, 0.0025 M, 0.005 M, 0.01 M) at 40 °C for 10 min to get final products. The as-prepared samples with different concentration of Cd(NO<sub>3</sub>)<sub>2</sub>·4H<sub>2</sub>O and TAA (0.001, 0.0025, 0.005, 0.01 M) are marked as CCFN/ZnO/CdS-X (X = 1, 2, 3, 4), respectively.

### 2.3 Photocatalytic activity test

In this experiment, 20 mg photocatalysts were added into 50 ml 1\*10<sup>-5</sup> mol/L rhodamine B (RhB) solutions in a quartz tube under the irradiation of visible light (PHILIPS,

500 W, λ ≥ 420 nm) with magnetic stirring during reaction. Before turning on the light, the reaction system was magnetically stirred in the dark for 30 min to reach the absorption–desorption equilibrium. The UV absorbance spectra of RhB solution for photocatalytic examination were collected every 30 min by UV–vis absorption spectrophotometer.

### 2.4 Characterization methods

The surface morphology and structure of the samples were investigated using Field-emission scanning electron microscope (FESEM, Hitachi S-4800) equipped with an Energy-dispersive X-ray spectroscopy (EDS), and transmission electron microscope (TEM, JEM-2100, 200 kV). Crystal structures of the samples were further characterized by X-ray diffraction (XRD, Bruker AXS D8-discover) with Cu-Kα line of 1.5418 Å. UV–vis absorption (U-3900 Hitachi equipped with a 30-mm integrating sphere) spectrophotometer was used to investigate ultraviolet performance property of the nanocomposite.

## 3 Results and discussion

Surface morphology of the CCFNs, CCFNs/ZnO seeds, CCFNs/ZnO nanorods and CCFNs/ZnO/CdS composite is shown in Fig. 1. Figure 1a reveals that CCFNs have uniform and smooth surfaces, with a diameter of about 100–200 nm. Figure 1b shows that dense and uniform ZnO seeds layer were successfully growth on CCFNs. As seen in Fig. 1c, the ZnO nanorods were successfully synthesized on the entire surface of CCFNs via the hydrothermal method. The length of the ZnO nanorods is about 1 μm, and the diameter is in the range of 70–80 nm. It is worth noting that the surface of the individual ZnO nanorod is smooth as shown in the inset of Fig. 1c. Figure 1d is the energy-dispersive X-ray (EDS) spectrum of the CCFNs/ZnO nanorods. It indicates that only C, O, and Zn existed in the EDS spectrum of CCFNs/ZnO nanocomposite, which further confirmed that the CCFNs/ZnO was successfully fabricated.

Figure 1e–h show the SEM images of the CCFNs/ZnO/CdS-X (X = 1, 2, 3, 4). It clearly indicates that CdS nanoparticles were successfully deposited on the surface of ZnO nanorods with the increase of precursor solution concentration from 0.001 M to 0.01 M. Figure 1h shows that more CdS nanoparticles were produced when the solution concentration is 0.01 M, which merge to form a continuous and uniform layer and almost cover the whole surface of the ZnO nanorods. As seen, the diameter of the CdS nanoparticles is in the range of 20–30 nm.

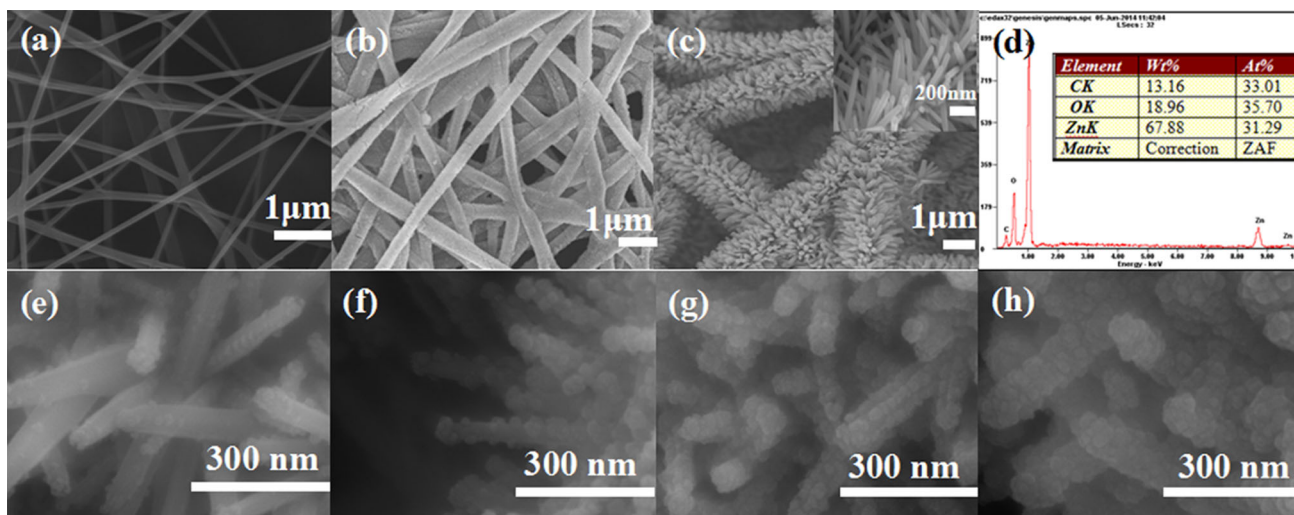


**Fig. 1** SEM images of the **a** CCNFs, **b** CCNFs/ZnO seed, **c** CCNFs/ZnO nanorods (the inset figure is greater magnification), **d** EDS spectrum of the CCNFs/ZnO, **e** CCNFs/ZnO/CdS-1, **f** CCNFs/ZnO/CdS-2, **g** CCNFs/ZnO/CdS-3, **h** CCNFs/ZnO/CdS-4

TEM and HRTEM measurements were performed to further characterize the morphology and structure of the CCNFs/ZnO/CdS-X. Figure 2a, b show that the ZnO nanorods are successfully covered by CdS nanoparticles, which proved that the precursor solution concentration is the main influencing factor for the amount of CdS nanoparticles on the ZnO nanorods. In addition, the HRTEM images of the ZnO and CdS were shown in Fig. 1e and f, respectively. The lattice spacing of 0.28 nm and 0.33 nm correspond to the hexagonal ZnO (101) plan and the face-centered cubic (fcc) CdS (002) plane, respectively.

The phase constitutions of the CCNFs/ZnO and CCNFs/ZnO/CdS-X were determined by XRD analysis (Fig. 3). Figure 3a shows the X-ray diffraction pattern of CCNFs/ZnO. The diffraction peaks can be indexed to the hexagonal ZnO (JCPDS99-0111). The patterns b, c, d and e obviously were indexed to hexagonal ZnO and fcc CdS (JCPDS 02-0454), which exhibit diffraction peaks corresponding to (111), (220) and (311) planes of the fcc structure of CdS, which corresponds to the HRTEM.

The optical absorption properties of CCNFs, CCNFs/ZnO and CCNFs/ZnO/CdS-X were measured by UV–vis absorption spectrometer. Figure 4 illustrates the UV–visible

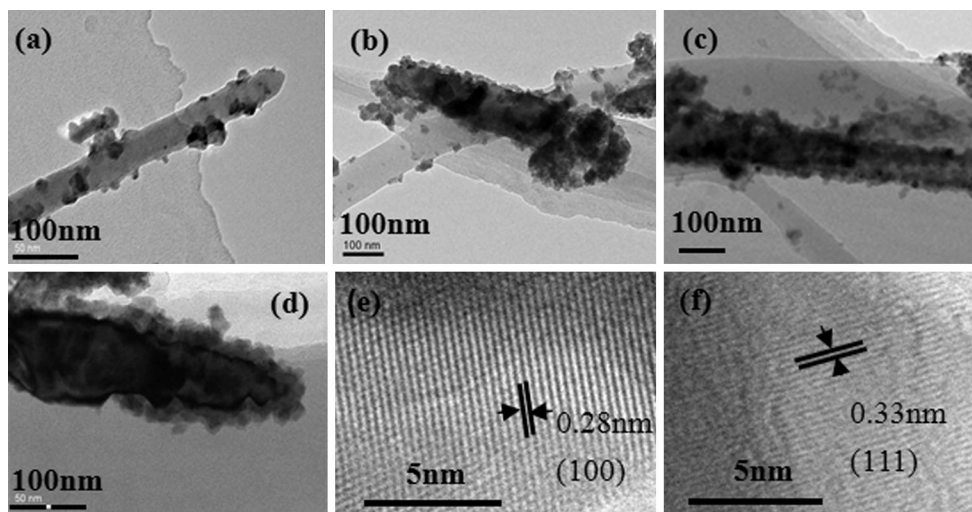


**Fig. 2** TEM images of the **a** CCNFs/ZnO/CdS-1, **b** CCNFs/ZnO/CdS-2, **c** CCNFs/ZnO/CdS-3, **d** CCNFs/ZnO/CdS-4, HRTEM images of the **e** ZnO and **f** CdS

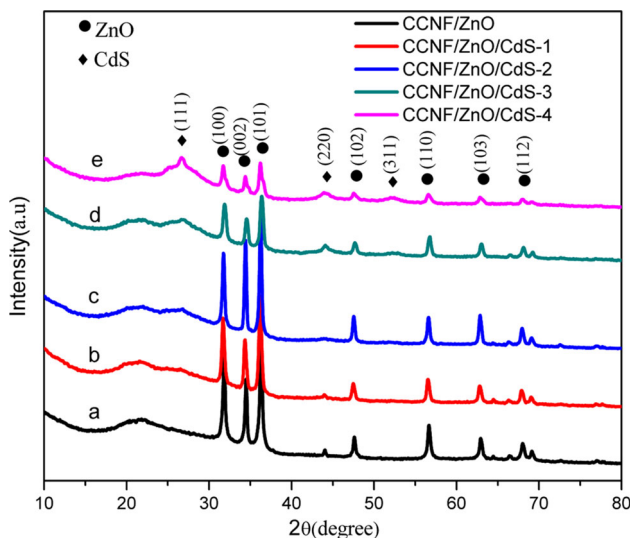


**Fig. 3** XRD patterns of the (a) CCFNs/ZnO, (b) CCFNs/ZnO/CdS-1, (c) CCFNs/ZnO/CdS-2, (d) CCFNs/ZnO/CdS-3, (e) CCFNs/ZnO/CdS-4

absorption spectra for CCFNs, CCFNs/ZnO and all the nanoscale hybrids with different loading of CdS. It is found that the as-prepared CCFNs/ZnO exhibits strong absorption in wavelengths shorter than 380 nm and no absorption in the visible light region, which is close to the value of bulk ZnO ( $E_{gZnO} = 3.37$  eV) [17]. Figure 4 clearly shows the absorption edge of CCFNs/ZnO/CdS-X has a significant red shift compared to CCFNs/ZnO, which is due to the increase in the CdS rod diameter then decrease the band gap energy ( $E_g$ ) of samples CCFNs/ZnO/CdS-1 through CCFNs/ZnO/CdS-4. As shown, a new photoabsorption in the visible region at the range of 400–700 nm appeared, which suggests that CdS indeed extended the light response range of the ZnO/CdS nanocomposite in the visible light region.

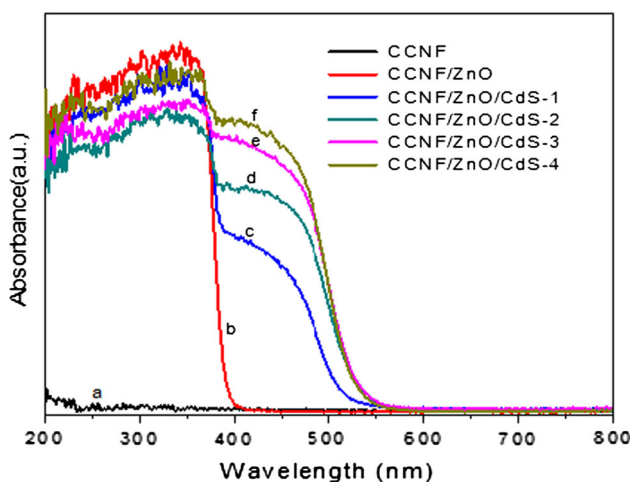


**Fig. 4** Ultraviolet visible absorption spectra of the (a) CCFNs, (b) CCFNs/ZnO, (c) CCFNs/ZnO/CdS-1, (d) CCFNs/ZnO/CdS-2, (e) CCFNs/ZnO/CdS-3, (f) CCFNs/ZnO/CdS-4

Photocatalytic activities of the samples were evaluated by measuring the degradation of RhB in aqueous solution under visible light irradiation. For comparison, the self-degradation of RhB under the irradiation of visible light without catalyst was measured (inset of Fig. 5a). The absorption spectrum of RhB solution almost has no change after irradiation for 180 min, which indicated that the self-degradation of RhB could be neglected. Figure 5a shows the UV–vis absorption spectrum of RhB aqueous solution with CCFNs/ZnO as photocatalyst during different time under the light irradiation exposure. As seen, the CCFNs/ZnO also has photocatalysis under visible light because RhB itself can sensitize ZnO [18]. The degradation efficiency of the samples is defined as  $(C_0 - C)/C_0$ , where  $C_0$  and  $C$  are the value of concentration of initial RhB and RhB after being decomposed, respectively. Figure 5b shows that the decolorization of RhB improve with the increasing CdS, (from CCFNs/ZnO/CdS-1 to CCFNs/ZnO/CdS-3), but the excess CdS (CCFNs/ZnO/CdS-4) will decrease the catalytic performance, which could be attributed to that the extensive CdS will be the center of electron–hole recombination [19]. In addition, the cycle catalytic performance was tested. Figure 5c shows that the CCFNs/ZnO/CdS-3 exhibits remarkable photostability with a slight decreasing after three cycles, which suggests that the photocatalytic activity of the CCFNs/ZnO/CdS-3 was stable and could effectively save the cost. The CCFNs/ZnO/CdS with excellent visible light catalysis performance is consider as a very promising material in the future.

On the basis of the experimental results and some other literatures [20–24], a mechanism for the effective photocatalytic activity of the CCFNs/ZnO/CdS is proposed. The schematic of the energy band structure and the charge-transfer process about the CCFNs/ZnO/CdS composite is shown in Fig. 6. As seen, CCFNs could increase the specific surface area of ZnO/CdS, which can increase the absorption of the visible light and the contact with the pollutants. In the photocatalytic process, CdS could absorb visible light to induce excited-state electrons and holes under visible light irradiation. The conduction band (CB) of CdS lies on more negative potential than that of ZnO, whereas the valence band (VB) of ZnO is more positive than that of CdS, which is helpful for the charge-transfer between ZnO and CdS. Electrons transfer from the CB of CdS transfer to that of the ZnO and holes on the VB of ZnO can transfer to that of the CdS. In brief, the heterojunction structure can promote the spatial separation of the electrons and holes. The separated holes will react with  $H_2O$  to generate  $\cdot OH$ . The separated electrons would subsequently react with  $H_2O$  and  $O_2$  to generate  $OH^-$  and  $O_2^{\cdot -}$ . And then, the radicals would oxidize the RhB efficiently due to their high oxidative capacity.

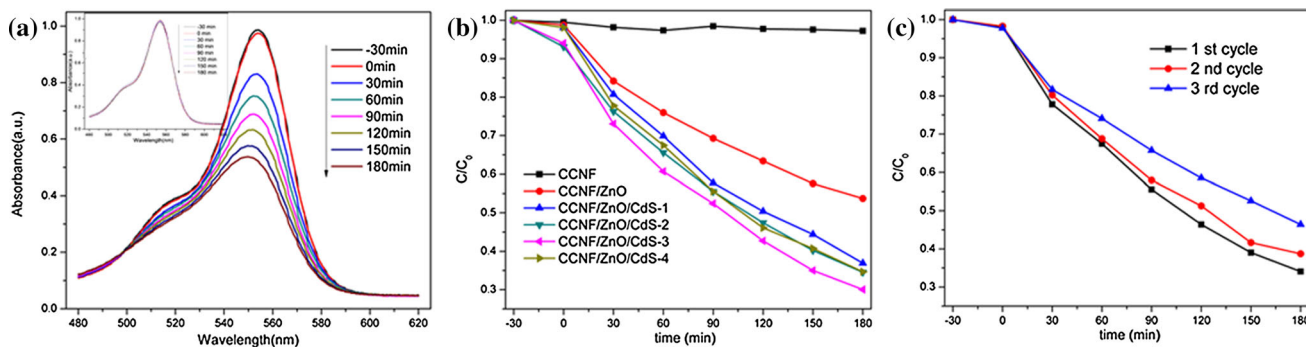


**Fig. 5** a UV–vis absorption spectra for degradation of RhB by using CCNFs/ZnO as photocatalyst. The inset shows the absorption spectrum of the RhB solution under visible light without any other

catalyst. b Curves of photocatalytic degradation on RhB with different photocatalyst. c Cyclic photodegradation curves of RhB with CCNFs/ZnO/CdS-3

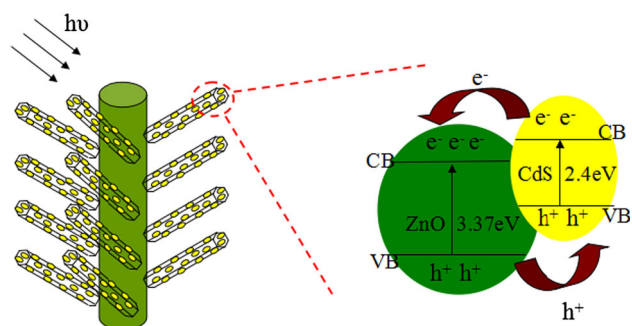


**Fig. 6** Schematic of the energy band structure and the charge-transfer process in the CCNFs/ZnO/CdS composite

### 4 Conclusions

In summary, a unique ternary photocatalyst CCNFs/ZnO/CdS composites has been successfully synthesized via electrospinning, hydrothermal and CBD method. The ZnO and CdS are hexagonal and face-centered cubic structure, respectively. The results indicates that the fabricated CCNFs/ZnO/CdS functional nanohybrid demonstrated a significantly enhanced photocatalytic activity compared to CCNFs/ZnO nanorods and the CCNFs/ZnO/CdS-3(0.005 M) has the best photocatalytic efficiency. For the CCNFs/ZnO/CdS functional nanocomposites, CCNFs play an important role in the recycling of the photocatalyst as the substrate material, ZnO serves as the main material, CdS, as a kind of visible light photosensitizer, successfully extended the light response range of the CCNFs/ZnO nanocomposites photocatalyst in the visible light region. The composites not only can bring new insight into the designing of highly efficient catalyst in environmental pollution control, but also have a great attractive for the solar cells applications.

**Acknowledgments** This work was supported by Natural Science Foundation of China (Nos. 51172209 and 91122022), and by the

Program for Changjiang Scholars and Innovative Research Team in University (PCSIRT) under Grant No. IRT13097, China.

### References

1. Y.N. Kuo, J. Hong, J. Colloid, Interface Sci. **285**, 232 (2005)
2. V.L. Pushparaj, M.M. Shaijumon, A. Kumar, S. Murugesan, L. Ci, R. Vajtai, R.J. Linhardt, O. Nalamasu, P.M. Ajayan, Proc. Natl. Acad. Sci. U.S.A. **104**, 13574 (2007)
3. B. Scrosati, Nat. Nanotechnol. **2**, 598 (2007)
4. L. Hu, H. Wu, F. La Mantia, Y. Yang, Y. Cui, ACS Nano **4**, 5843 (2010)
5. P. Andersson, D. Nilsson, P.-O. Svensson, M. Chen, A. Malmström, T. Remonen, T. Kugler, M. Berggren, Adv. Mater. **14**, 1460 (2002)
6. H. Gullapalli, V.S. Vemuru, A. Kumar, A. Botello-Mendez, R. Vajtai, M. Terrones, S. Nagarajiah, P.M. Ajayan, Small **6**, 1641 (2010)
7. D.-H. Kim, Y.-S. Kim, J. Wu, Z. Liu, J. Song, H.-S. Kim, Y.Y. Huang, K.-C. Hwang, J.A. Rogers, Adv. Mater. **21**, 3703 (2009)
8. K.Y. Lee, B. Kumar, J.S. Seo, K.H. Kim, J.I. Sohn, S.N. Cha, D. Choi, Z.L. Wang, S.W. Kim, Nano Lett. **12**, 1959 (2012)
9. C.R. Li, R. Chen, X.Q. Zhang, J. Xiong, Y.Y. Zheng, W.J. Dong, Fiber. Polym. **12**, 345 (2011)
10. C.R. Li, S.X. Shu, R. Chen, B.Y. Chen, W.J. Dong, J. Appl. Polym. Sci. **130**, 1524 (2013)
11. Q. Liu, J. Li, Y. Zhao, Y. Zhou, C. Li, Mater. Lett. **138**, 89 (2015)
12. T. Rakshit, S.P. Mondal, I. Manna, S.K. Ray, A.C.S. Appl. Mater. Interfaces **4**, 6085 (2012)
13. A.B. Martinson, M.S. Goes, F. Fabregat-Santiago, J. Bisquert, M.J. Pellin, J.T. Hupp, J. Phys. Chem. A **113**, 4015 (2009)
14. P. Charoensirithavorn, T. Sagawa, J. Sol. Energy Eng. **133**, 011101 (2011)
15. W.T. Sun, Y. Yu, H.Y. Pan, X.F. Gao, Q. Chen, L.M. Peng, J. Am. Chem. Soc. **130**, 1124 (2008)
16. G. Wang, X. Yang, F. Qian, J.Z. Zhang, Y. Li, Nano Lett. **10**, 1088 (2010)
17. R. Demir, S. Okur, M.E. Şeker, M. Zor, Ind. Eng. Chem. Res. **50**, 5606 (2011)
18. V. Srikant, D.R. Clarke, J. Appl. Phys. **83**, 5447 (1998)
19. J. Yang, C. Chen, H. Ji, W. Ma, J. Zhao, J. Phys. Chem. B **109**, 21900 (2005)
20. T.C. Dang, D.L. Pham, H.C. Le, V.H. Pham, Adv. Nat. Sci. Nanosci. Nanotechnol. **1**, 015002 (2010)

21. G. Yang, W. Yan, Q. Zhang, S. Shen, S. Ding, *Nanoscale* **5**, 12432 (2013)
22. X.W. Wang, G. Liu, Z.G. Chen, F. Li, L.Z. Wang, G.Q. Lu, H.-M. Cheng, *Chem. Commun.* **23**, 3452 (2009)
23. S.R. Lingampalli, U.K. Gautam, C.N.R. Rao, *Energy Environ. Sci.* **6**, 3589 (2013)
24. J.D. Zhuang, W.X. Dai, Q.F. Tian, Z.H. Li, L.Y. Xie, J.X. Wang, P. Liu, X.C. Shi, D.H. Wang, *Langmuir* **26**, 9686 (2010)